Recovery of methane from a variable-volume bed of silica sand/hydrate by depressurization

ARTICLE *in* ENERGY & FUELS · MARCH 2010

Impact Factor: 2.79

4 AUTHORS, INCLUDING:

Praveen Linga
National University of Singapore
92 PUBLICATIONS **1,786** CITATIONS
SEE PROFILE

Peter Englezos
University of British Columbia - Vancouver
182 PUBLICATIONS **4,838** CITATIONS
SEE PROFILE

John A. Ripmeester
National Research Council Canada
716 PUBLICATIONS **15,772** CITATIONS
SEE PROFILE

Recovery of methane from a variable-volume bed of silica sand/hydrate by depressurization

Haligva, Cef; Linga, Praveen; Ripmeester, John A.; Englezos, Peter

Publisher's version / la version de l'éditeur:
Energy and Fuels, 24, 5, pp. 2947-2955, 2010-04-14

Web page / page Web
http://dx.doi.org/10.1021/ef901220m
http://nparc.cisti-icist.nrc-cnrc.gc.ca/npsi/ctrl?action=rtdoc&an=17673443&lang=en
http://nparc.cisti-icist.nrc-cnrc.gc.ca/npsi/ctrl?action=rtdoc&an=17673443&lang=fr

Energy Fuels **2010,** *24,* 2947–2955 · DOI:10.1021/ef901220m
Published on Web 04/14/2010

energy&fuels
article

Recovery of Methane from a Variable-Volume Bed of Silica Sand/Hydrate by Depressurization

Cef Haligva,[†] Praveen Linga,[†] John A. Ripmeester,[‡] and Peter Englezos*[,†]

[†]*Department of Chemical and Biological Engineering, University of British Columbia, Vancouver, British Columbia, Canada V6T 1Z3, and* [‡]*Steacie Institute for Molecular Sciences, National Research Council of Canada, Ottawa, Ontario, Canada K1A 0R6*

Received October 26, 2009. Revised Manuscript Received April 1, 2010

Methane hydrate was formed in water occupying the interstitial spaces of a cylindrical bed of silica sand particles. The sand particles have an average diameter equal to 329 μm. The amount of methane consumed during the experiment (methane gas uptake) was determined through pressure and temperature measurements and mass balance calculations. Three different sized beds of silica sand particles were used. Water conversion to hydrates in the range of 73−84% was achieved for all of the formation experiments. Hydrate formation was followed by decomposition at 4.0 °C driven by depressurization at 3.1 MPa (nine experiments) and 2.3 MPa (one experiment). Methane recovery measurement curves were determined for each experiment. The initial rate of recovery was found to be strongly dependent on the silica sand bed size. The rate of recovery was found to depend weakly on the size during the second stage, and after 1.25 h, it was constant. During decomposition at 2.3 MPa, the temperature in some locations inside the bed dropped below the freezing point of water and the gas recovery rate was enhanced. This is in agreement with recently reported conclusions by Tsypkin [*Fluid Dynamics* **2005**, *40* (1), 117−125] and Zhou et al. [*Ind. Eng. Chem. Res.* **2009**, *48* (6), 3142−3149]. Finally, the gas recovery data was correlated with an empirical model with one parameter that was found to depend linearly on the bed size.

1. Introduction

Efforts to extract natural gas from naturally occurring gas hydrates in the Earth date back to the early 1980s.[3−8] It is estimated that natural gas trapped in solid gas hydrates in the Earth represents a potentially huge resource.[9−12] Holder et al.[13] concluded that the decisive factors that enable a gas hydrate reservoir to produce gas efficiently are the reservoir porosity and the thermal properties of the hydrates and reservoir. Other than these factors, knowledge of the rate of hydrate decomposition is also required. In order to assess the feasibility of producing natural gas from the Earth's hydrates, reservoir-specific information, together with laboratory data and models, is needed.[14]

*To whom correspondence should be addressed. Tel: 1-604-822-6184. Fax: 1-604-822-6003. E-mail: englezos@interchange.ubc.ca.

(1) Tsypkin, G. G. Effect of decomposition of a natural gas hydrate on gas recovery from a reservoir containing hydrate and gas in the free state. *Fluid Dynamics* **2005**, *40* (1), 117–125.
(2) Zhou, Y.; Castaldi, M. J.; Yegulalp, T. M. Experimental Investigation of Methane Gas Production from Methane Hydrate. *Ind. Eng. Chem. Res.* **2009**, *48* (6), 3142–3149.
(3) Davidson, D. W.; El-Defrawy, M. K.; Fuglem, M. O.; Judge, A. S. Natural Gas Hydrates in Northern Canada. *Int. Conf. Permafrost Proc.* **1978**, *3* (1), 937–943.
(4) Bowsher, A. L. Proceedings of a Workshop on Clathrates in NPRA held in Menlo Park 7/16-17/79. USGS Open File Report, 1981, 81-1298, 0-164.
(5) Stoll, R. D.; Bryan, G. M. Physical Properties of Sediments Containing Gas Hydrates. *J. Geophys. Res.* **1979**, *84* (B4), 1629.
(6) Barraclough, B. L. Methane Hydrate Resource Assessment Program. Los Alamos Science Laboratory Progress Report No. LA-8569-PR; April−June 1980; p 27.
(7) Makogon, Y. F. Perspectives for the Development of Gas-Hydrate Deposits. *4th Can. Permafrost Conf. Proc. R.J.E. Brown Memor. Volume* **1982**, 299–304.
(8) Judge, A. Natural Gas Hydrates in Canada. *4th Can. Permafrost Conf. Proc. R.J.E. Brown Memor. Volume* **1982**, 320–328.
(9) Klauda, J. B.; Sandler, S. I. Global distribution of methane hydrate in ocean sediment. *Energy Fuels* **2005**, *19* (2), 459–470.
(10) Kvenvolden, K. Potential effects of gas hydrate on human welfare. *Proc. Natl. Acad. Sci. U.S.A.* **1999**, *96*, 3420.
(11) Makogon, Y. F.; Holditch, S. A.; Makogon, T. Y. Natural gas-hydrates—A potential energy source for the 21st Century. *J. Pet. Sci. Eng.* **2007**, *56* (1−3), 14–31.
(12) Milkov, A. V.; Claypool, G. E.; Lee, Y. J.; Xu, W. Y.; Dickens, G. R.; Borowski, W. S. In situ methane concentrations, at Hydrate Ridge, offshore Oregon: New constraints on the global gas hydrate inventory from an active margin. *Geology* **2003**, *31* (10), 833–836.
(13) Holder, G. D.; Angert, P. F.; John, V. T.; Yen, S. A Thermodynamic Evaluation of Thermal Recovery of Gas from Hydrates in the Earth. *J. Pet. Technol.* **1982**, *34* (5), 1127–1132.
(14) Kneafsey, T. J.; Tomutsa, L.; Moridis, G. J.; Seol, Y.; Freifeld, B. M.; Taylor, C. E.; Gupta, A. Methane hydrate formation and dissociation in a partially saturated core-scale sand sample. *J. Pet. Sci. Eng.* **2007**, *56* (1−3), 108–126.
(15) Moridis, G.; Collett, T. S.; Dallimore, S. R.; Satoh, T.; Hancock, S.; Weatherill, B. Numerical Simulation Studies of Gas Production Scenarios From Hydrate Accumulations at the Mallik Site, Mackenzie Delta, Canada. *Proceedings of the 4th International Conference on Gas Hydrates*, May 19−23, 2002, Yokohama, Japan; 2002; Keio University: Yokohama, pp 239−244.
(16) Moridis, G. J. Numerical studies of gas production from methane hydrates. *SPE J.* **2003**, *8* (4), 359–370.
(17) Moridis, G. J.; Kowalsky, M. B. Response of oceanic hydrate-bearing sediments to thermal stresses. *SPE J.* **2007**, *12* (2), 253–268.
(18) Gerami, S.; Pooladi-Darvish, M. Predicting gas generation by depressurization of gas hydrates where the sharp-interface assumption is not valid. *J. Pet. Sci. Eng.* **2007**, *56* (1−3), 146–164.
(19) Kowalsky, M. B.; Moridis, G. J. Comparison of kinetic and equilibrium reaction models in simulating gas hydrate behaviour in porous media. *Energ. Convers. Manage.* **2007**, *48* (6), 1850–1863.
(20) Moridis, G. J. Numerical studies of gas production from Class 2 and Class 3 hydrate accumulations at the Mallik site, Mackenzie Delta, Canada. *SPE Reservoir Eval. Eng.* **2004**, *7* (3), 175–183.
(21) Moridis, G. J.; Collett, T. S.; Dallimore, S. R.; Satoh, T.; Hancock, S.; Weatherill, B. Numerical studies of gas production from several CH_4 hydrate zones at the Mallik site, Mackenzie Delta, Canada. *J. Pet. Sci. Eng.* **2004**, *43* (3−4), 219–238.

Despite the efforts and progress achieved on the topic of modeling and simulation,[15−21] there are only a small number of articles on hydrate formation and decomposition kinetics in porous media.[2,14,22−26]

Selim and Sloan[26] found that the rate of hydrate dissociation induced by thermal stimulation depends on the thermal properties and the porosity of the reservoir. Yousif and Sloan[27] concluded that the gas production behavior during hydrate dissociation depends on the amount of hydrate formed, the uniformity of the hydrates along the core, and the difference between the dissociation pressure and the equilibrium pressure (driving force).

Handa and Stupin[22] reported thermodynamic properties and dissociation characteristics of methane and propane in 70 Å silica gel pores. Handa and Stupin[22] reported that the equilibrium pressures were 20−100% higher than those of the bulk hydrates. Also on the basis of dissociation by heating of the hydrates at zero pressure from 100 K to room temperature, Handa and Stupin[22] found that the hydrate trapped in the interior of the pore remained stable up to the melting point of pore ice. Stern et al.[23] observed the irregularities of methane clathrate hydrate formation and solid-state deformation. These observations were made at conditions lower than 105 K and 10^{-3} Pa, whereas the naturally occurring hydrates exist at approximately 3−10 MPa and above-freezing temperatures.[14]

Tang et al.[25] concluded that the amount of gas produced by the thermal stimulation of an unconsolidated sediment increases with time until a maximum is reached and then starts to decrease. Kneafsey et al.[14] formed and dissociated methane hydrate within silica sand in an X-ray transparent pressure vessel in which the temperature, pressure, and local density changes were monitored. The dissociation of hydrate was induced by depressurization coupled with thermal stimulation. They observed formation of a low-density rind between the vessel and the sample (sand + water + hydrate) during hydrate formation. They also concluded that heat transfer and the relative permeability are affected by the degree of saturation of the phases present, and these properties are, in turn, affected by water movement. Zhou et al.[2] studied hydrate formation/decomposition in a water-saturated silica sand matrix. The particle size of the sand was in the range of 100−500 μm. The experiments were conducted at 2.2 °C and 4137 kPa in a 72 L vessel. The authors reported water conversion to hydrate of 11% for the formation experiment and employed depressurization to release the gas.

One aspect that was not examined in previous laboratory studies with synthetic hydrate samples or samples recovered from the Earth is the impact of the sample size on the rate with which the gas is consumed during hydrate formation or released during hydrate dissociation. Recently, Linga et al.[28,29] reported data on methane hydrate formation and dissociation in a bed of silica sand particles saturated with water. The average diameter of the sand particles was 329 μm. Linga et al.[28] reported water conversion to hydrate in the range of 74−98% for all experiments conducted at 4.0 °C and at a pressure of 8.0 MPa. The occurrence of multiple nucleation events and the spatial heterogeneity of hydrate formation resulted in hydrate formation occurring at three distinguishable rates during the experiment. When the hydrate was decomposed by thermal stimulation, it was found that the methane release (recovery) per mole of water proceeds in two stages. The dissociation was found to depend on the size of the bed during the first stage of dissociation.[29]

Dissociation of hydrate by pressure reduction along with thermal stimulation are regarded as the most likely approaches for implementation in naturally occurring hydrate reservoirs. Thus, it is of interest to examine whether the size of the laboratory sample affects the rate of recovery of methane during depressurization. Hence, the objective of this work was to study the kinetics of hydrate decomposition via depressurization in the apparatus described by Linga et al.[28,29] This apparatus was specifically designed to investigate the potential dependence of the rate of gas recovery on the size of the laboratory hydrate sample. This work completes the investigation.

2. Experimental Section

2.1. Materials. Ultra-high-purity-grade methane (Praxair Technology Inc.) and distilled/deionized water were used. The silica sand used in this study (Sigma Aldrich) was the same sand as that used by Linga et al.[28,29] The silica sand has an average diameter of 329 μm, a specific internal pore volume of 0.000 152 $cm^3\ g^{-1}$, and an average internal pore diameter of 0.9 nm.[28,29]

2.2. Apparatus. A brief description of the apparatus is given here because the complete description is available elsewhere.[28] The apparatus consisted of a cylindrical stainless steel crystallizer (CR) and a reservoir immersed in a temperature-controlled water bath. The temperature profiles of the hydrate phase and the gas phase were measured using Omega copper/constantan thermocouples with an uncertainty of 0.1 K. Four thermocouples were inserted in various locations of the bed and one in the gas phase. A thermocouple was also placed in the water bath. The pressure in the crystallizer and reservoir and the temperature data were recorded using a data acquisition system coupled with *LabView 8.0* software. The control valve connected between the crystallizer and reservoir communicates with the PID controller and allows the transfer of the gas between the crystallizer and reservoir during the decomposition experiment.

In order to study the effect of the variable volume of the silica sand bed on hydrate decomposition, two copper cylinders were placed inside the crystallizer. This reduced the bed size while the resistance to heat transfer was minimized. Both copper cylinders fit precisely in the crystallizer, and there was no gap between the crystallizer wall and the copper cylinders, as illustrated by Linga et al.[28] The first copper cylinder (CC_1) had an inner diameter of 7.62 cm (3 in.), and the second one (CC_2) had an inner diameter of 5.08 cm (2 in.). The wall thickness of both cylinders was 1.27 cm (0.5 in.). Four thermocouples were inserted in the silica bed, with both CC_1 and CC_2 present in the crystallizer. Figure 1

(22) Handa, Y. P.; Stupin, D. Thermodynamic Properties and Dissociation Characteristics of Methane and Propane Hydrates in 70A Radius Silica Gel Pores. *J. Phys. Chem.* **1992**, *96*, 8599.
(23) Stern, L. A.; Kirby, S. H.; Curham, W. B. Peculiarities of Methane Clathrate Hydrate Formation and Solid-State Deformation, Including Possible Superheating of Water Ice. *Science* **1996**, *273* (5283), 1843–1848.
(24) Katsuki, D.; Ohmura, R.; Ebinuma, T.; Narita, H. Methane hydrate crystal growth in a porous medium filled with methane-saturated liquid water. *Philos. Mag.* **2007**, *87* (7), 1057–1069.
(25) Tang, L. G.; Xiao, R.; Huang, C.; Feng, Z. P.; Fan, S. S. Experimental investigation of production behavior of gas hydrate under thermal stimulation in unconsolidated sediment. *Energy Fuels* **2005**, *19* (6), 2402–2407.
(26) Selim, M. S.; Sloan, E. D. Hydrate Dissociation in Sediment. *SPE Reservoir Eng.* **1990**, 245.
(27) Yousif, M. H.; Sloan, E. D. Experimental investigation of hydrate formation and dissociation in consolidated porous media. *SPE Reservoir Eng.* **1991**, *6* (4), 452–458.
(28) Linga, P.; Haligva, C.; Nam, S. C.; Ripmeester, J. A.; Englezos, P. Gas hydrate formation in a variable volume bed of silica sand particles. *Energy Fuels* **2009**, *23* (11), 5496–5507.
(29) Linga, P.; Haligva, C.; Nam, S. C.; Ripmeester, J. A.; Englezos, P. Recovery of methane from hydrate formed in a variable volume bed of silica sand particles. *Energy Fuels* **2009**, *23* (11), 5508–5516.

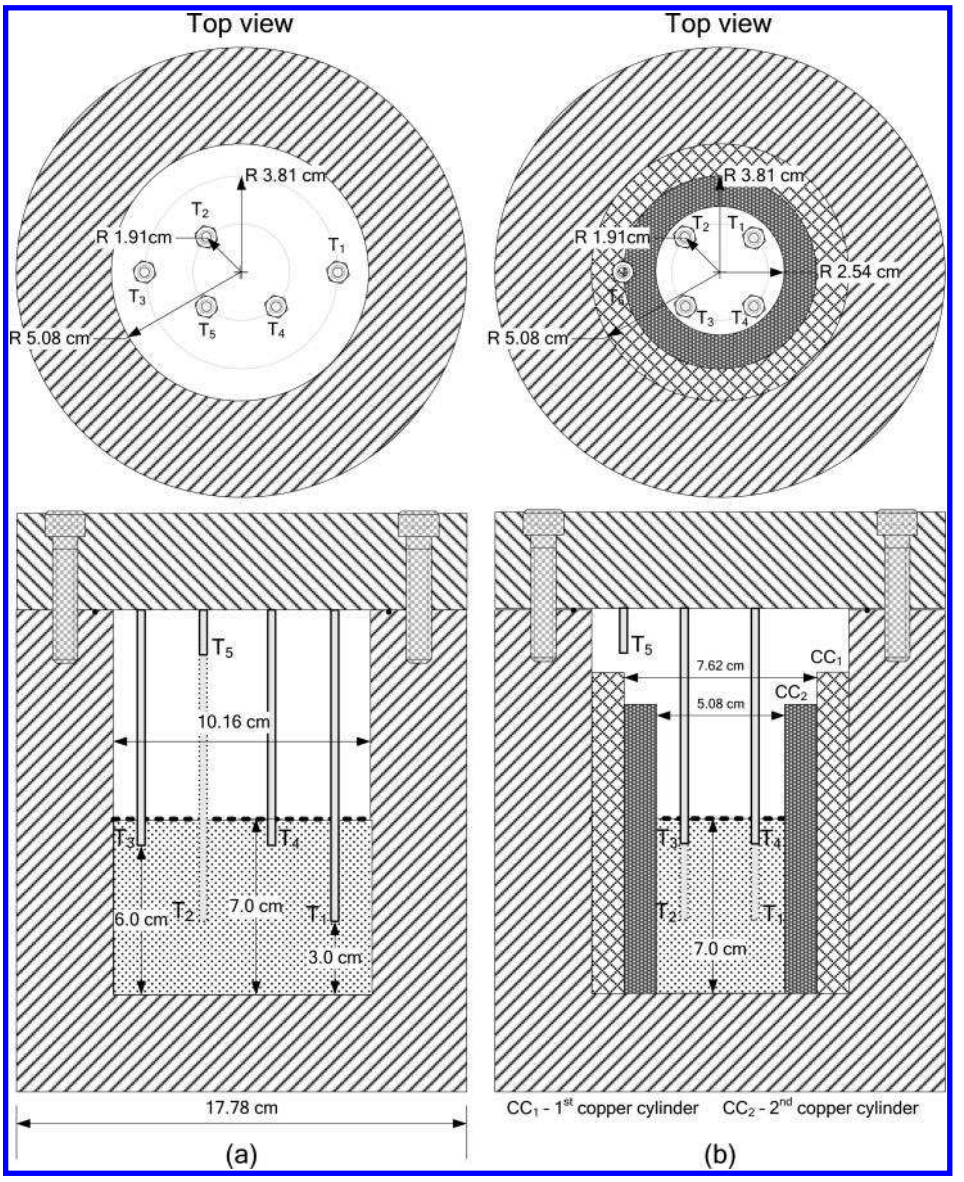

Figure 1. Cross section of the crystallizer showing (a) the location of the thermocouples within the crystallizer without the copper cylinders and (b) the arrangement of the copper cylinders (CC_1 and CC_2) in the crystallizer and the location of the thermocouples (adapted from Linga et al.[28]).

shows the schematic (top and cross-sectional views) of the thermocouples placed in the crystallizer with and without the presence of copper cylinders.

2.3. Procedure for Hydrate Formation. The experimental procedure for the formation is described in detail by Linga et al.[28] Briefly, the amount of silica sand put in the crystallizer was 914.1 g. The porosity of the sand bed was determined to be 0.35.[28] The volume of water required to fill the void space (100% water saturation) was found to be 0.217 $cm^3\ g^{-1}$, which is the interstitial or pore volume of the bed of sand particles. Accordingly, 198.5 mL of water was added to the sand. The procedure for the formation experiment was the same when one (CC_1) or two copper cylinders ($CC_1 + CC_2$) were placed in the crystallizer. However, the amount of the sand placed in the crystallizer was reduced to 513.7 g when there was one (CC_1) copper cylinder present inside the crystallizer, and the amount of water added to fill the void space of the sand was 111.7 mL. When two ($CC_1 + CC_2$) copper cylinders were present, the amounts of sand and water added were 228.5 g and 49.7 mL, respectively. For all three cases, the height of the sand + water bed was 7 cm.

The bed was set up by splitting the required amount of sand and water into five equal parts and placing each in a batch order (sand + water) to form a uniform bed and also to eliminate the presence of any pockets of air in the bed.[28] Once the crystallizer bed was set up, then the crystallizer was closed and the thermocouples were positioned. The crystallizer was pressurized with methane and depressurized at a pressure below the equilibrium hydrate formation pressure three times in an attempt to eliminate the presence of any air bubbles in the system. The pressure in the crystallizer was then set to the desired experimental pressure and the formation experiment was started. All hydrate formation experiments were carried out at constant temperature, and the system operated as a closed one. The experiment was allowed to continue until a time when there was no significant change in the crystallizer pressure.

2.4. Procedure for Hydrate Decomposition by Depressurization. After completion of each hydrate formation experiment, the pressure was brought down to a value corresponding to about 10% above the equilibrium pressure. The equilibrium pressure, P_{eq}, at 4.0 °C was 3.85 MPa, as calculated using CSMHYD (Sloan[30]). Thus, for our experiments, this pressure

(30) Sloan, E. D., Jr. *Clathrate Hydrates of Natural Gases*, 2nd ed., revised and expanded; Marcel Dekker: New York, 1998; p 754.

Table 1. Hydrate Formation Induction Times, Water Conversion to Hydrate, Hydrate Decomposition Pressure, and Methane Recovery[a]

		formation experiment				decomposition experiment	
			end of the experiment				
system	exp. no.	induction time [min]	time [h]	CH_4 consumed [mole of gas (mol of H_2O)$^{-1}$]	water conversion to hydrates [mol %]	P_{exp} [MPa]	methane recovery [mol %]
CH_4/silica sand/water [CR]	1	363.0	56.1	0.1256	76.6	3.1	97.8
	2	39.7	49.8	0.1228	74.9	3.1	95.6
	3	332.7	72.6	0.1199	73.2	3.1	95.8
CH_4/silica sand/water [CR + CC_1]	4	17.0	89.1	0.1203	73.4	3.1	94.3
	5	2.7	77.2	0.1256	76.6	3.1	96.4
	6	15.7	74.7	0.1255	76.6	3.1	93.1
CH_4/silica sand/water [CR + CC_1 + CC_2]	7	206.7	167.8	0.1377	84.0	3.1	94.2
	8	92.3	161.2	0.1228	74.9	3.1	94.8
	9	4.0	108.3	0.1232	75.2	3.1	93.9
	10	246.0	119.1	0.1251	76.3	2.3	80.6

[a] The initial experimental pressure for all of the formation experiments was 8.0 MPa. All experiments were conducted at 4.0 °C.

was 4.2 MPa (3.85 + 0.385). The temperature in the crystallizer was then allowed to stabilize. Obviously, at this pressure the hydrate was still thermodynamically stable. Subsequently, the pressure in the crystallizer was reduced to the experimental decomposition pressure of 3.1 MPa. The average rate of pressure reduction for all of the experiments was 10.1 ± 2.6 kPa s^{-1}. Once the pressure in the crystallizer reached the set point, this was time zero for the decomposition experiment. It was observed through an increase in the pressure in the collection reservoir that hydrates started to decompose immediately. Because the pressure in the crystallizer was maintained constant at 3.1 MPa by a PID controller coupled with a control valve, the excess gas released from the crystallizer due to hydrate decomposition was collected in the reservoir (R). The experiment was stopped when there was no further release of methane gas.

The procedure to calculate the amount of methane gas consumed as a result of hydrate formation and methane gas released from hydrate decomposition was described by Linga et al.[28,29] The percent methane recovery was calculated as a function of time for any given decomposition experiment based on the information obtained from its formation experiment and was calculated by the following equation:

$$\%\ \text{methane recovery} = \frac{(\Delta n_{H,\uparrow})_t}{(\Delta n_{H,\downarrow})_{t_{end}}} \times 100 \qquad (1)$$

where $(\Delta n_{H,\uparrow})_t$ is the number of moles of methane released from hydrates during hydrate decomposition at any given time and $(\Delta n_{H,\downarrow})_{t_{end}}$ is the number of moles of methane consumed for hydrate formation at the end of a formation experiment.

The rates of hydrate decomposition (methane release) were calculated for all of the kinetic experiments conducted using the forward difference method given as

$$\left(\frac{dn}{dt}\right)_t = \frac{n_{t+\Delta t} - n_t}{\Delta t}, \quad \Delta t = 20\ \text{s} \qquad (2)$$

The average of theses rates over 30 min (90 rate datum points) was computed, and this was reported as the average rate of hydrate decomposition (R_{av})

3. Results and Discussion

3.1. Gas Hydrate Formation for Depressurization Experiments. Table 1 summarizes the hydrate formation experimental conditions and results indicating the induction time and water-to-hydrate conversion achieved. All of the formation experiments were conducted at a temperature (T_{exp}) of 4.0 °C and at a pressure of 8.0 MPa at the start of the experiment. The conversion of water to hydrate was determined for all of the formation experiments and is presented in Table 1. The hydration number for the methane/water system was assumed to be 6.1 for our calculations.[31] For all of the formation experiments that were carried out at different silica sand bed sizes, water-to-hydrate conversions of ~73% and above were achieved. The induction times shown in the table vary considerably as expected because of the stochastic nature of hydrate nucleation.

Figure 2 shows a typical gas uptake curve and the temperature profile within the bed during the formation experiment (experiment 1). As can be observed in the figure, there are multiple sudden temperature increases at the same location, which indicates that a number of nucleation events happen along with hydrate growth. The first temperature increase (first nucleation point) can be seen in section B in the figure appearing at 363 min (6.05 h). The first hydrate nucleation occurs at approximately the same time (within 1.0 min) in the four thermocouple locations [more precisely, T_2, T_3, and T_4 at 363 min (6.05 h) and T_1 at 364 min (6.07 h)]. In section C, the temperature increase is not localized and a largest rate of gas consumption occurs. Several temperature spikes are seen in the other time periods (sections D−F), which indicates that nucleation occurs at several sites throughout the bed volume. Hence, hydrate formation happens at different locations at different times and at different rates, similar to what was observed and reported by Linga et al.[28] As discussed in detail in our previous work,[28] this multiplicity of hydrate nucleation occurring at different times in the bed was considered to be responsible for achieving a high percent conversion of water to hydrate.[28]

3.2. Gas Hydrate Decomposition by Depressurization. The experimental conditions for decomposition and the corresponding results are summarized in Table 1. Experiments 1−9 were conducted at a decomposition pressure of 3.1 MPa, whereas experiment 10 was carried out at 2.3 MPa. A typical gas recovery curve obtained from the decomposition experiment conducted at 3.1 MPa is shown in Figure 3. Recall that time zero coincides with the time when the pressure in the crystallizer reaches 3.1 MPa (start of the decomposition experiment). Methane release occurs immediately from time zero because the pressure and temperature of the system are outside the equilibrium conditions for methane hydrate. Methane release from hydrate for this experiment lasted 15 h. As explained in the Experimental Section, before the

(31) Tulk, C. A.; Ripmeester, J. A.; Klug, D. D. The application of Raman spectroscopy to the study of gas hydrates. *Gas Hydrates: Challenges for the Future*; New York Academy of Sciences: New York, 2000; Vol. 912, pp 859−872.

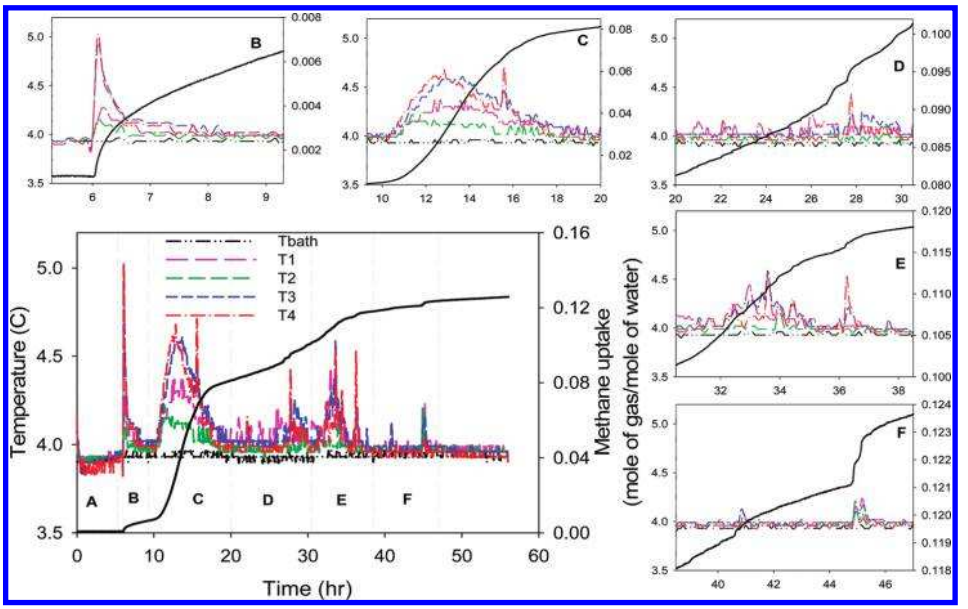

Figure 2. Gas uptake measurement curve (experiment 1).

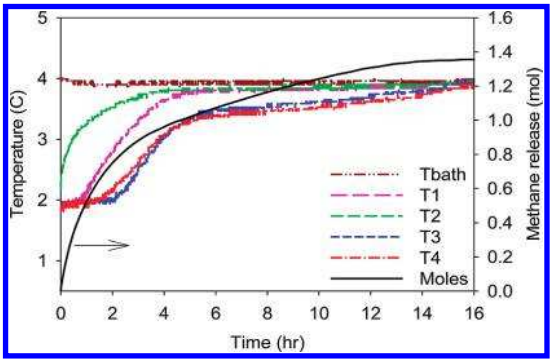

Figure 3. Methane release curve along with the temperature profiles inside the bed (T_1, T_2, T_3, and T_4) and in the water bath (T_{bath}) during decomposition by depressurization carried out at 3.1 MPa (experiment 1).

start of the decomposition experiment, the pressure in the crystallizer was reduced from 4.2 to 3.1 MPa (P_{exp}). During this step, the temperature inside the crystallizer dropped dramatically because of the sudden pressure release from the constant-volume reactor. For the experiments conducted at 3.1 MPa, the average temperature drop at the thermocouples due to pressure release from 4.1 to 3.1 MPa was found to be 2.0 (±0.2) °C. It is noted that the equilibrium temperature was calculated using CSMHYD (Sloan[30]) and found to be 1.8 °C at 3.1 MPa. Because the external temperature (T_{bath}) was kept constant at 4.0 °C, the temperature profiles inside the crystallizer eventually reached 4.0 °C, as seen in Figure 3. There are two heat effects that would determine the rate at which the temperature is restored to the set temperature of 4.0 °C. The first is the control system that aims to maintain a temperature of 4.0 °C. The second is the heat effect associated with the dissociation of hydrate. The relative magnitude of these effects is expected to differ from one thermocouple to another. It should be noted that hydrate formation in the silica sand bed/water matrix is spatially and temporally heterogeneous in nature, as discussed in detail by Linga et al.[28] Consequently, the temperature trajectory for each thermocouple will also reflect the signature left by the hydrate formation process locally. The impact of the temperature and pressure profiles before the start of the decomposition experiment is discussed later in this section.

Figure 4 shows the temperature profiles and methane release curves for two experiments obtained with one copper cylinder, CC_1 (experiment 6), and two copper cylinders, $CC_1 + CC_2$ (experiment 8). The methane release for experiment 6 was complete in 9 h, while the methane release for the experiment with the smallest bed size (experiment 8) finished in 3.5 h. The location of thermocouple T_4 is the same as that for all of the bed sizes (Figure 2). For the largest bed size (CR), T_4 reaches the experimental temperature of 4.0 °C in ~16 h (Figure 3), while it takes 8 h (Figure 4, top) when one copper cylinder is placed in the crystallizer and ~2 h (Figure 4, bottom) when two copper cylinders are placed in the crystallizer (CR + CC_1 + CC_2). This is probably due to the fact that the resistance to heat transfer by the copper cylinder is much smaller compared to that by the sand/hydrate/water matrix and the amount of heat required to decompose the smaller hydrate samples will be less than that required for the larger samples. The thermal conductivity of copper is 400 W m^{-1} K^{-1}.[32] The thermal conductivities of water[32] and hydrate[33] are 0.58 and 0.5 W m^{-1} K^{-1}, respectively. The thermal conductivity of sand[32] is assumed to be equal to that of quartz, 1.4 W m^{-1} K^{-1}.

The average rate of hydrate decomposition (R_{av}) for the three experiments conducted with the smallest bed size (CR + CC_1 + CC_2) is shown in Figure 5. As seen, the rates are quite high in the first 0.5 h (0.35 mol h^{-1}), then decrease with time [1 h (0.14 mol h^{-1}) and 1.5 h (0.07 mol h^{-1})], and gradually approach zero as the methane recovery is completed within 4 h. This trend was observed for the experiments conducted for the other two bed sizes. Figures S1 and S2 given in the Supporting Information represent the rate of methane release for the other two bed sizes.

Figure 6 shows a comparison of the percent methane recovery curves (calculated using eq 1) for all of the decomposition

(32) Incropera, F. P.; DeWitt, D. P. *Fundamentals of Heat and Mass Transfer*, 5th ed.; John Wiley & Sons Inc.: New York, 2002.

(33) Cook, J. G.; Leaist, D. G. An Exploratory Study of the Thermal Conductivity of Methane Hydrate. *Geophys. Res. Lett.* **1983**, *10* (5), 397–399.

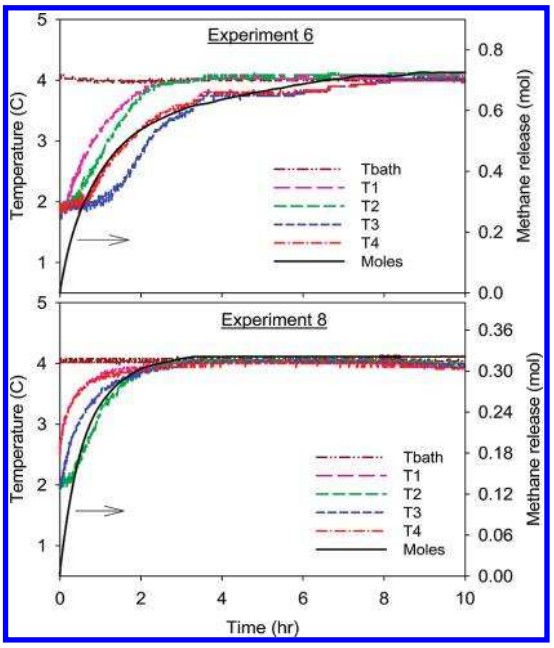

Figure 4. Methane release curve along with the temperature profiles during decomposition by depressurization carried out at 3.1 MPa.

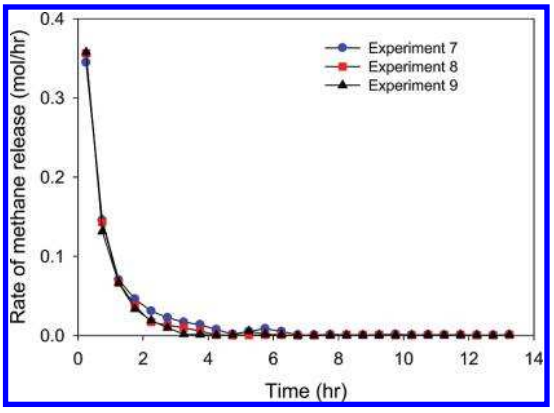

Figure 5. Average rate of methane release for the three experiments conducted with two copper cylinders present in the crystallizer ($CR + CC_1 + CC_2$).

experiments carried out by the depressurization method and for all three cases: one with a silica bed at its largest size (CR), one with a silica sand bed with one copper cylinder ($CR + CC_1$) inside the crystallizer, and one silica sand bed with both copper cylinders ($CR + CC_1 + CC_2$) placed in the crystallizer. It can be seen in the figure that the duration of methane recovery becomes shorter as the bed size decreases. For the largest bed size (CR), the recovery is completed in 14 h, for the medium bed size ($CR + CC_1$), the recovery is completed in 9 h, and for the smallest bed size ($CR + CC_1 + CC_2$), the recovery is completed in 4 h. When the bed size is reduced, less water is present and hence less hydrate is formed prior to decomposition experiments, leading to less methane release. Consequently, methane recovery is completed faster. It is recalled that the height of the bed was kept the same for all three cases (7 cm). Thus, the qualitative nature of the recovery curves is preserved as the bed diameter decreases by installing copper cylinders inside the crystallizer. Although quantitatively the curves are not identical (different dynamics), the final percent recoveries are almost the same.

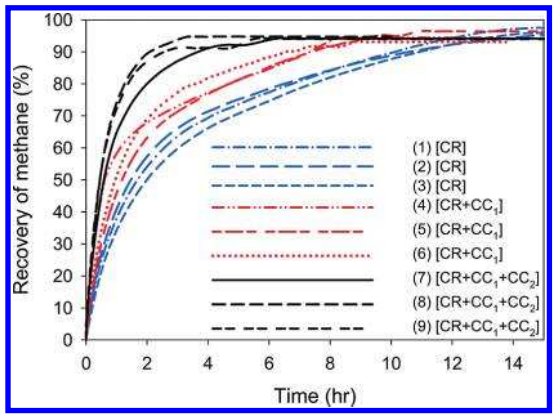

Figure 6. Comparison of the percent methane recovery from decomposition by depressurization experiments for three different silica bed sizes (CR, $CR + CC_1$, $CR + CC_1 + CC_2$). The numbers in parentheses indicate the experiment numbers in Table 1.

The data in Figure 6 are fitted with the following equation:

$$\frac{R}{R_{eq}} = 1 - \exp(-t/\mu) \qquad (3)$$

where R is the percent methane recovery at time t, R_{eq} is the percent methane recovery at the end of the experiment, and μ is a time constant. Table 2 shows the optimum values of the parameter (μ) along with the minimized objective function and the standard deviation of the estimated parameter. The parameters were regressed using the Luus–Jaakola[34,35] optimization procedure, and the data were regressed simultaneously (three experiments of each bed size) in order to get a global time constant for each bed size. The estimated time constants were 3.13, 1.75, and 0.74 h for the three experimented bed sizes. The standard deviation of the estimated optimum parameter was less than 2%. Interestingly, there is a linear relationship between the estimated time constant for the three bed sizes, as shown in Figure 7. As reported in Table 2, one experiment was conducted at 2.3 MPa. The value of the time constant for that experiment was 0.16 h, which was significantly lower compared to the value (0.74 h) obtained from experiments conducted at 3.1 MPa.

The rates of methane release per mole of water were also determined because the beds hold different amounts of water, which is available for hydrate formation. Figure 8 shows the calculated rates of methane release per mole of water plotted as a function of time for the three bed sizes. The average rates of recovery for the three experiments conducted for each bed size (CR, $CR + CC_1$, and $CR + CC_1 + CC_2$) are presented along with the standard deviation. There is a decreasing trend in the calculated rate of methane release for all three bed sizes, and the rates reach a plateau at about 4 h and eventually become zero when the recovery is complete. It is also evident from the figure that there is a strong dependence of the rate of methane release on the bed size for the first two time periods (from 0 to 0.5 h and from 0.5 to 1.0 h), and then the rates are more or less the same from the third time period (from 1.0 to 1.5 h) and thereafter. As one can see, the rates of recovery for the first time period

(34) Luus, R.; Jaakola, T. H. I. Optimization by Direct Search and Systematic Reduction of Size of Search Region. *AIChE J.* **1973**, *19* (4), 760–766.

(35) Linga, P.; Al-Saifi, N.; Englezos, P. Comparison of the Luus–Jaakola optimization and Gauss–Newton methods for parameter estimation in ordinary differential equation models. *Ind. Eng. Chem. Res.* **2006**, *45* (13), 4716–4725.

Table 2. Objective Function and Optimum Parameter Values along with Its Standard Deviation for the Three Bed Sizes

system	objective function (least squares)	parameter, time constant, μ [h]	standard deviation of the parameter [%]
CR	0.8455	3.13	1.39
CR + CC_1	0.8493	1.75	1.97
CR + CC_1 + CC_2	0.1428	0.74	1.26
CR + CC_1 + CC_2[a]	0.0199	0.16	1.92

[a] Experiment 10, depressurization experiment conducted at 2.3 MPa.

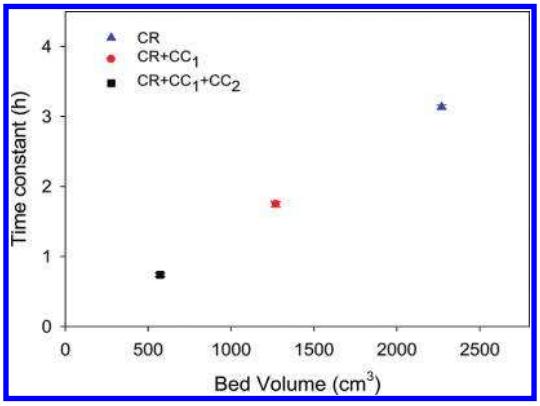

Figure 7. Estimated time constant plotted against the three bed size experiments, showing a linear relationship.

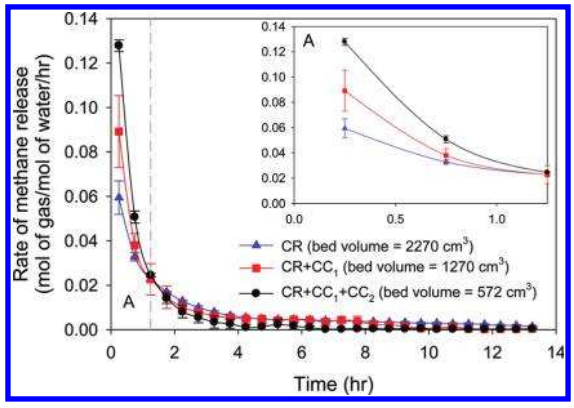

Figure 8. Comparison of the rates of methane recovery for the three different bed sizes (the average and standard deviation of the three experiments are reported in the figure). Region A is expanded and presented as an inset in the figure.

(from 0 to 0.5 h) are strongly affected by the bed size. As we narrow down the bed size, the rate of recovery increases significantly. During the second time period (from 0.5 to 1.0 h), the rate increases, but slightly, as the bed size decreases. It can be seen from Figure 6 that, at about 1.5 h, ~45% of methane is recovered in the largest bed size (2270 cm^3), ~60% of methane is recovered in the medium bed size (1270 cm^3), and ~80% of methane is recovered in the smallest bed size (572 cm^3). So even though the rates of methane recovery (%) at 1.5 h for the three bed sizes are significantly different, the rates of methane release at 1.5 h seem to be the same. Recently, Linga et al.[29] reported a similar dependence of the sample size on the recovery rates for the first stage based on the thermal stimulation approach for two different driving forces of 4.0 and 10.0 °C, respectively. Hence, when laboratory experimental data are used to compare models utilizing adjustable parameters, it is prudent to employ data with different sample sizes. Although we have not examined samples from naturally occurring gas

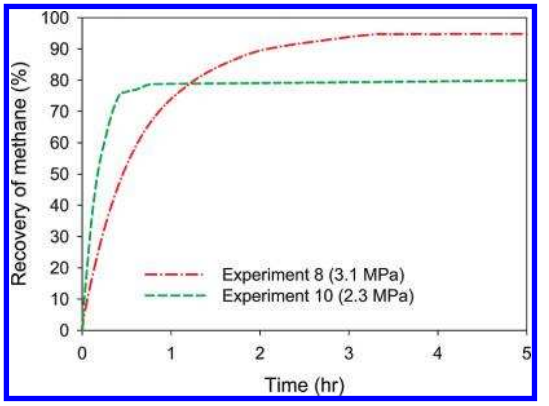

Figure 9. Recovery percentage comparison between depressurization experiments conducted at 3.1 and 2.3 MPa.

hydrates, it would be of interest to obtain different sample sizes for physical testing when the rate of gas release is measured.

One decomposition experiment was performed at a lower pressure of 2.3 MPa. Figure 9 shows a comparison of methane recovery (%) for the experiment conducted at 2.3 MPa (experiment 10) and an experiment conducted at 3.1 MPa (experiment 8). The recovery is much faster when we increase the driving force of depressurization as expected. However, the recovery at the end of the experiment conducted at 2.3 MPa was only 80.6%, whereas for the experiment conducted at 3.1 MPa, it was 94.8%. This is because of the gas release due to hydrate decomposition occurring while the crystallizer pressure is being reduced from 4.2 to 3.1 MPa before the start of the decomposition experiment. Therefore, there is some gas released that could not be captured in the reservoir.

The temperature and pressure profiles for a typical experiment (experiment 2) just before the start of the decomposition experiment (predecomposition step) are shown in Figure 10. The solid lines in the pressure curve (Figure 10, bottom) are the actual pressure readings inside the crystallizer. In this figure, projected pressure values are shown with the dashed line (calculated by fitting a straight line to the pressure data from the time that the pressure reduction started to go up to P_{eq}). As can be seen in the figure, if the hydrate did not start to decompose at the moment that the equilibrium pressure (3.85 MPa) point is reached during the depressurization process, the pressure line would have followed the dotted line shown in the figure. However, as the pressure in the system is reduced below the equilibrium pressure (3.85 MPa), the decomposition starts and hence the pressure reduction rate slows down by the time the desired experimental pressure is reached. The amount of gas lost during this step was estimated by converting the difference in the pressure drop into the number of moles and was found to be 2.1% for experiment 2. For all of the experiments conducted at 3.1 MPa, the amount of gas lost

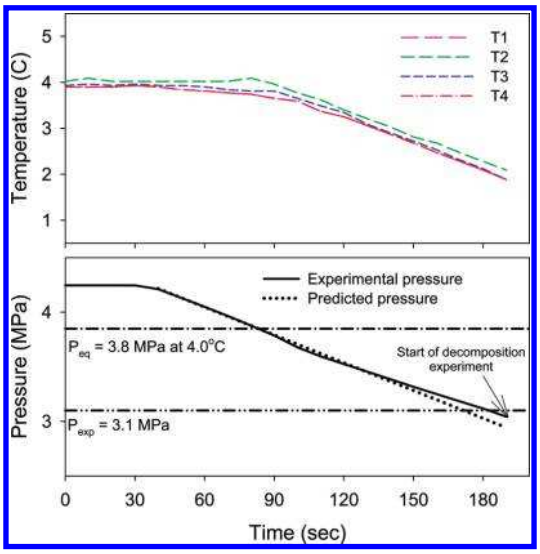

Figure 10. Temperature and pressure profiles during predecomposition gas release from 4.2 to 3.1 MPa and the projected pressure reduction for experiment 2.

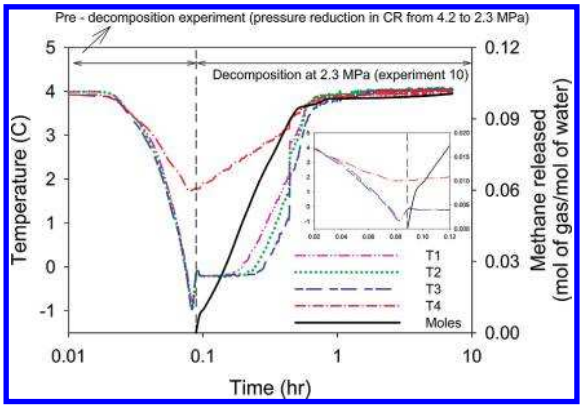

Figure 11. Methane release curve for experiment 10 also indicating the temperature profile before the start of the decomposition experiment when the pressure in the crystallizer was reduced from 4.2 to 2.3 MPa (P_{exp}). Note that the x axis is presented as a logarithmic scale and time zero of the actual experiment is indicated by a vertical dashed line and the x axis for the figure in the inset is presented as a linear scale for better visualization of the results.

was found to be 1−4%. When the pressure was reduced for a longer period of time, as for the 2.3 MPa experiment, the amount of gas lost before the start of the decomposition experiment that cannot be captured in the reservoir was higher. Hence, it is not surprising that the recovery percentage for the experiment conducted at 2.3 MPa (experiment 10) was lower compared to the experiments conducted at 3.1 MPa. On the basis of the foregoing discussion, we decided not to perform experiments at 2.3 MPa for the other bed sizes so that the amount of gas lost during depressurization was kept at a minimum although the rate of recovery was significantly faster if decomposition was carried out at 2.3 MPa.

The temperature profile during the predecomposition step when the pressure in the crystallizer was reduced from 4.1 to 2.3 MPa (experiment 10) can be seen in Figure 11. During the pressure reduction step, the temperature at thermocouple locations T_1, T_2, and T_3 dropped from 4.0 to −0.9 (±0.1) °C, whereas the temperature at thermocouple location T_4 dropped from 4.0 to 1.8 °C. The temperatures at T_1, T_2, and T_3 quickly

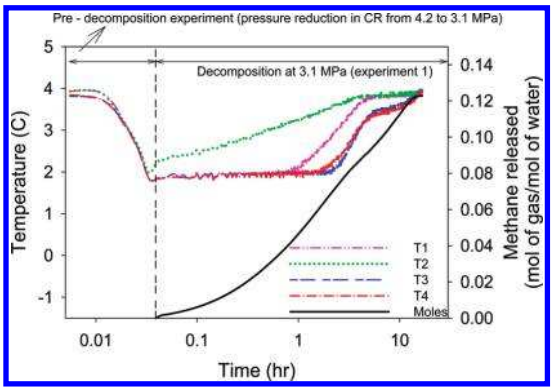

Figure 12. Methane release curve for experiment 1 also indicating the temperature profile before the start of the decomposition experiment when the pressure in the crystallizer was reduced from 4.2 to 3.1 MPa. Note that the x axis in the figure is presented as a logarithmic scale and time zero of the actual experiment is indicated by a vertical dashed line.

(0.0055 h) reached ∼0.0 °C and stayed there for about 0.16, 0.24, and 0.25 h, respectively. After that, they gradually reached the experimental setpoint temperature of 4.0 °C. This step (temperature increase from −0.9 to ∼0.0 °C) also resulted in increased gas recovery, as seen in the figure (shown as an inset). Tsypkin[1] predicted that it is possible that hydrate may dissociate into water and ice simultaneously (in addition to gas). Tsypkin[1] also showed theoretically that an increased amount of gas may be produced when this happens. Zhou et al.[2] recently confirmed experimentally that the increased gas production is due to decomposition into ice and liquid water. Our results at 2.3 MPa (experiment 10) independently confirm the increased gas production (Figure 12) when the temperature dropped below the freezing point. It is noted that our decomposition experiment was conducted at a constant pressure of 2.3 MPa, while the experiment conducted by Zhou et al.[2] was not conducted at constant pressure. Interestingly, during the experiments conducted at 3.1 MPa, the temperature did not drop below the freezing point and an enhanced gas recovery was not observed. The relevant data for experiment 1 are illustrated in Figure 12. As seen in the figure, the temperature dropped only to about 1.9 °C during the pressure reduction from 4.1 to 3.1 MPa. The average temperature reduction for all of the experiments (experiments 1−9) conducted at 3.1 MPa was 2.0 (±0.2) °C. It is noted that the equilibrium temperature for methane hydrate formation at 3.1 MPa is 1.8 °C.[30]

4. Conclusions

Methane hydrate was formed in three different size beds of silica sand/water matrix and was subsequently decomposed by depressurization. A high percentage conversion of water to hydrates (73.2−84%) was achieved for all of the experiments conducted in this study. For the decomposition experiments conducted at 3.1 MPa and for the three bed sizes, the behavior of the recovery rate could be classified as distinguishable during two time periods. The rate during the first time period (from 0 to 0.5 h) depends strongly on the size of the bed. There is a weak dependence on the size during the second time period (from 0.5 to 1.0 h) and the rates are more or less the same thereafter. The recovery was found to be much faster for the decomposition experiment conducted at 2.3 MPa compared to the experiments conducted at 3.1 MPa. For the decomposition experiment conducted at 2.3 MPa, it was observed that the temperature

inside the bed at some locations dropped below the freezing point of water and in which the gas recovery was enhanced. Finally, a one-parameter empirical model was found to fit the gas recovery data.

Acknowledgment. Financial support from the Natural Sciences and Engineering Research Council of Canada (NSERC) and Natural Resources Canada (NRCan) is greatly appreciated.

Appendix

Nomenclature

n = number of moles
$(\Delta n_{H,\downarrow})_{t_{end}}$ = number of moles consumed for hydrate formation at the end of a formation experiment
$(\Delta n_{H,\uparrow})_t$ = number of moles released from hydrates during hydrate decomposition at any given time
P_{eq} = equilibrium pressure at a given temperature
R_{av} = average rate of hydrate formation for 30 min
R = percent recovery of hydrate at any given time
R_{eq} = percent recovery of hydrate at the end of the experiment
μ = time constant (h)

Supporting Information Available: Rate of methane release with no copper cylinders, CR (Figure S1), and rate of methane release with one copper cylinder, CR + CC_1 (Figure S2). This material is available free of charge via the Internet at http://pubs.acs.org.